Appl. Phys. B (2013) 112:185–192
DOI 10.1007/s00340-013-5415-4

Applied Physics B
Lasers and Optics

Theoretical and experimental study of single mode-locking pulse generation with low repetition rate in a dual-loss-modulated QML YVO_4/Nd:YVO_4 laser with EO and GaAs

H. J. Zhang · S. Z. Zhao · K. J. Yang · G. Q. Li · D. C. Li · J. Zhao

Received: 12 November 2012 / Accepted: 12 March 2013 / Published online: 28 March 2013

Abstract Using electro-optic (EO) modulator and GaAs saturable absorber, a diode-pumped doubly Q-switched and mode-locked (QML) YVO_4/Nd:YVO_4 laser at 1.06 μm is realized. The experimental results show that the number of the mode-locking pulses underneath the Q-switched envelope decreased with increasing pump power. With an output coupling of 6.5 %, the single mode-locking pulse underneath the Q-switched envelope with 1 kHz repetition rate was obtained when the pump power exceeded 4.65 W. At a pump power of 8.25 W for an output coupling of 10 %, a stable mode-locking pulse train at a repetition rate of 1 kHz was achieved with pulse energy as high as 582 μJ and pulse duration of about 580 ps, corresponding to a peak power of 1 MW. Using a hyperbolic secant square function and considering the Gaussian distribution of the intracavity photon density, the coupled rate equations for diode-pumped doubly QML YVO_4/Nd:YVO_4 laser are given and the numerical solutions of the equations are basically in accordance with the experimental results.

1 Introduction

Ultra-short pulse lasers with great pulse energy, high peak power and low repetition rate have found wide applications in the fields of ultrafast spectroscopy [1], biological medicine [2, 3], micromachining [4, 5] and ophthalmic surgery [6]. In fluorescence lifetime measurement, the maximal measurable lifetime depends strongly on the repetition rate of the laser system, and a decrease of the repetition rate can greatly increase the range of measurable lifetimes. Continuous wave (CW) mode-locking technology can generate stable ultra-short laser pulses with duration in fs and ps regimes, but the generated pulse repetition rate is generally very high (typically from MHz to GHz) [7–9]. In order to reduce the repetition rate of mode-locking pulses, some efforts have been paid. By increasing the cavity length, Kolev et al. [10] and Kobtsev et al. [11] reduced the repetition rate to 1.5 and 77 kHz in a mode-locked Nd:YVO_4 laser and a mode-locked fiber laser, respectively. By introducing a pulse picker, Balzer et al. [12] reduced the repetition rate to 340 kHz in a mode-locked semiconductor laser system. In spite of complicated laser systems in the above-mentioned methods, it is also difficult to obtain the low repetition rate of several KHz.

Simultaneously, Q-switched and mode-locking (QML) process involves two dynamic processes related to Q-switching and mode-locking, so it is considered as a transition state from Q-switching to mode-locking regimes. For the QML lasers, the mode-locked pulses underneath the Q-switched envelope have sub-nanosecond duration while the Q-switched envelope has kHz repetition rate and tens of nanoseconds pulse width typically. Generally, there are many mode-locking pulses in a Q-switched envelope. Since the QML pulses have large fluctuations in amplitude, the application fields of these QML lasers are limited. By employing the dual-loss-modulated QML method, i.e., with active modulator and passive saturable absorber simultaneously, stable QML pulse envelopes with high energy and optional repetition rates can be generated [13–16]. Because the interval of two mode-locked pulses is equal to the cavity round-trip transmit time, the shorter the pulse width of the Q-switched envelope is, the less the number of

H. J. Zhang · S. Z. Zhao (✉) · K. J. Yang · G. Q. Li · D. C. Li · J. Zhao
School of Information Science and Engineering, Shandong University, 27 Shanda South Road, 250100 Jinan, China
e-mail: shengzhi_zhao@sdu.edu.cn

mode-locked pulses in a Q-switched envelope is. Most important, the dual-loss-modulated QML regime can apparently reduce the duration of the Q-switched envelope, which also depends on the pump power, the small-signal transmission of the saturable absorber, the laser gain medium, the repetition rate of the active modulator and so on [16]. By choosing appropriately related parameters, shorter pulse width of the Q-switched pulse envelope can be possibly obtained. In such a way, it is expected to realize single mode-locked pulse underneath the Q-switched envelope, which has duration in sub-nanosecond regime and low repetition rate at several kHz.

Due to the excellent properties such as wide absorption bandwidth at 808 nm (21 nm), large stimulated emission cross-section (25×10^{-19} cm^2) [5, 17, 18], Nd:YVO_4 crystal has been widely investigated in continuous wave, Q-switching, and mode-locking lasers, which have also been applied in broad areas of scientific research, industry, medicine, etc. However, the thermal effect of Nd:YVO_4 crystal is detrimental to the lasing operation, thus affects the output characteristics including output power, stability and beam quality, etc. Thermal diffusion bonding technique can be used to bond the non-doped and doped crystals with the same host together. Owing to the heat sink effect of the non-doped crystal, the temperature gradient between the center and side face of laser crystal was effectively weakened, resulting in the attenuation of the thermal lens effect caused by end deformation, and thus the laser stability would be improved. The employment of a composite crystal YVO_4/Nd:YVO_4 has been demonstrated to be an effective method of relieving the thermal lens effect [19].

In this paper, a diode-pumped dual-loss-modulated QML YVO_4/Nd:YVO_4 laser with an EO modulator and a GaAs saturable absorber is presented. For this doubly QML laser, the pulse width of the Q-switched envelope decreased with the increase of the pump power, resulting in less number of the mode-locking pulses underneath the Q-switched envelope. When the pump power exceeded 4.65 W for an output coupling of $T = 6.5$ %, single mode-locking pulse operation underneath the Q-switched envelope was obtained. This single mode-locking pulse train had a repetition rate of 1 kHz determined by the EO modulator, and the measured mode-locking pulse width was about 580 ps. When the pump power was 8.25 W for an output coupling of $T = 10$ %, a maximum peak power of the single mode-locking pulse is estimated to be about 1 MW. By considering the Gaussian transversal distribution of the intracavity photon density and the longitudinal distribution of the photon density along the cavity axis, the coupled rate equations for a diode-pumped doubly QML YVO_4/Nd:YVO_4 laser with an EO modulator and a GaAs saturable absorber are given. These coupled rate equations were solved numerically. The dependence of pulse energy and pulse width of the Q-switched envelope on the incident pump power and the output coupler transmission was obtained. The calculated temporal shapes of the mode-locking pulses for the output coupling of 6.5 % were also given. The theoretically numerical simulations are basically in accordance with the experimental results.

2 Experiment

2.1 Experimental setup

The experimental setup is depicted in Fig. 1. The pump source was a commercial fiber-coupled laser diode (Coherent, FAP system), which worked at the maximum absorption wavelength (808 nm) of the Nd^{3+} ions. The pump light was focused into the YVO_4/Nd:YVO_4 sample by two coupling lenses with a 4-cm focal length. The focused pump beam in the laser medium had an average diameter about 400 μm. The laser host was an a-cut YVO_4/Nd:YVO_4 composite crystal with a dimensions of $4 \times 4 \times (3 + 8)$ mm^3 which was fabricated by the thermal diffusion bonding technique. The Nd:YVO_4 in composite crystal had a Nd^{3+} doping concentration of 0.5 at %. One end facet of the Nd:YVO_4 crystal was antireflective (AR) coated at 1,064 nm, while the other end facet of YVO_4 was AR coated at 808 and 1,064 nm, acting as the pump end. The laser crystal was wrapped with a thin layer of indium foil and mounted in a copper holder cooled by a thermo-electric cooler. The folded laser cavity consisted of three mirrors. Concave mirror M_1 with the radius of curvature (ROC) of 150 mm was AR coated at 808 nm and high-reflection (HR) coated at 1,064 nm. The folded concave mirrors M_2 with the ROC of 500 mm was HR coated at 1,064 nm. M_3 was a plane output mirror. In the experiment, three output couplers with different transmission of $T = 6.5$, 10, and 15 % were employed. An EO modulator (BBO crystal, the repetition rate 1–5 kHz) with a polarizer and λ/4 plate was employed as active Q-switcher while a GaAs wafer with small-signal transmission of 92.6 % was

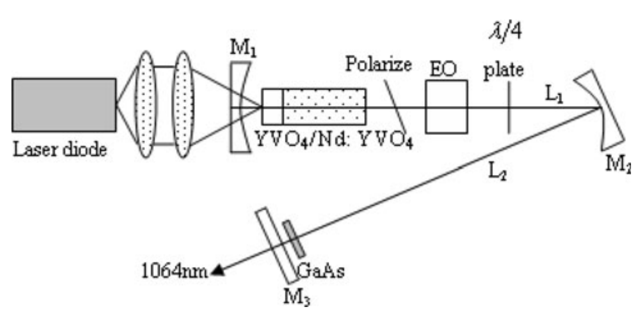

Fig. 1 Dual-loss-modulated QML YVO_4/Nd:YVO_4 laser setup

used as passive saturable absorber. Since short Q-switched pulse can be generated at lower repetition of the active modulator [15, 16], the EO modulator was set at 1 kHz. The lengths of the two cavity arms, L_1 and L_2 were 600 and 460 mm, respectively. According to the ABCD matrix theory, the average radius of the TEM00 mode oscillating in the cavity w_l, the radii of TEM00 mode at the positions of gain medium and GaAs wafer w_G and w_A were estimated to be about 200, 206, and 132 μm. The pulse characteristics were recorded by a digital oscilloscope (8 GHz bandwidth and 40 G samples/s sampling rate, Agilent, USA) and a fast pin photodiode detector with a rise time of 0.4 ns. A laser power meter (MAX 500AD, Coherent, USA) was employed to measure the average output power.

2.2 Experimental results

For the dual-loss-modulated QML laser with active modulator and passive saturable absorber, the repetition rate of the Q-switched envelope depends on the active modulation rate. Figure 2 shows the average output power of the QML laser and the pulse energy of the Q-switched envelope versus incident pump power with different output couplers. The pulse energy was calculated according to the average output power and the repetition rate. When the pump power was about 7.09 W and T = 15 %, a maximum average output power of 692 mW was obtained.

The dependences of the pulse widths of the Q-switched envelope on the pump power are shown in Fig. 3, from which it can be observed that the pulse width of the Q-switched envelope decreases with increasing pump power. Because the time interval between two neighboring mode-locking pulses underneath the Q-switching envelope is equal to $2L'/c$, where L' is the optical length of the laser resonator and c is the speed of the light, shorter Q-switched envelope results in less number of mode-locking pulses underneath the Q-switching envelope. When the pump power exceeded 4.65 W for the output couplings of T = 6.5 % and 5.94 W for T = 10 %, respectively, the pulse widths of the Q-switched envelope were shorter than $2L'/c$. This means that single mode-locking pulse underneath a Q-switching envelope was obtained, i.e., a mode-locking pulse train with a repetition rate of 1 kHz was achieved. However, it should be noted that there was no such phenomenon of single mode-locking pulse underneath the Q-switching envelope when an output coupler of T = 15 % was employed.

To demonstrate the change of the mode-locking pulse number underneath Q-switched envelope more directly and conveniently, some pulses recorded by the oscilloscope for the output coupling of T = 6.5 % are shown in Fig. 4, in which (a), (b), (c), and (d) correspond to four different pump powers. Figure 4a, b shows that the Q-switched and

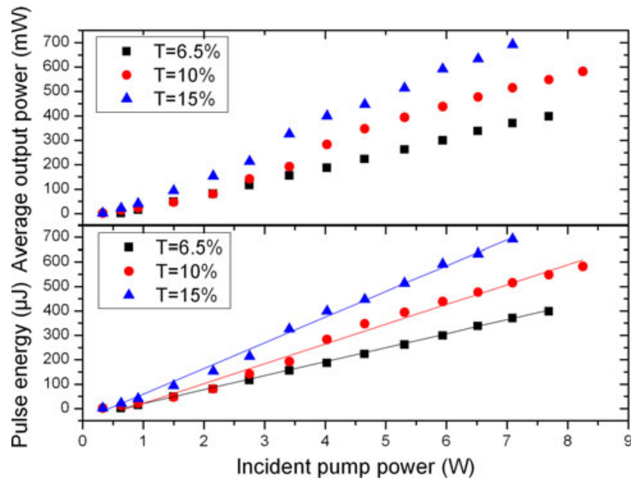

Fig. 2 Average output power (*upper part*) of QML laser and pulse energy (*lower part*) of the Q-switched envelope on the incident pump power. *Symbol* experimental data, *solid curve* theoretical result

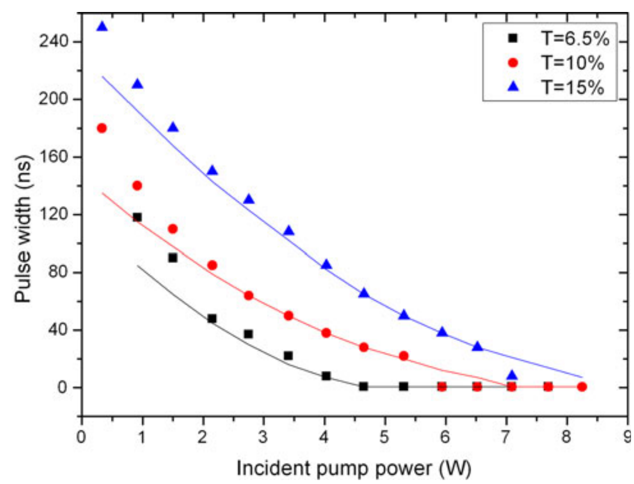

Fig. 3 Pulse width of Q-switched envelope versus incident pump power. *Symbol* experimental data, *solid curve* theoretical result

mode-locking pulse trains have a small DC level, which may be caused by the dark current of the photodiode detector and the optical noise of background. When the pump power was 2.75 W, there were six mode-locking pulses underneath one Q-switched envelope. When the pump power was 4.03 W, only two mode-locking pulses existed. When the pump power reached 4.65 W, there was only one mode-locking pulse underneath a Q-switching envelope. Figure 5 shows the expanded images of the above mentioned four mode-locking pulse trains recorded in Fig. 4. The measured mode-locking pulse durations were 1.1 ns, 900 ps, and 580 ps at the pump power of 2.75, 4.03, and 4.65 W, respectively. This indicates that the mode-locking pulse duration also decreases with the increase of the incident pump power. In addition, there was no obvious relationship between the mode-locking pulse duration and the output coupler transmission in the experiment.

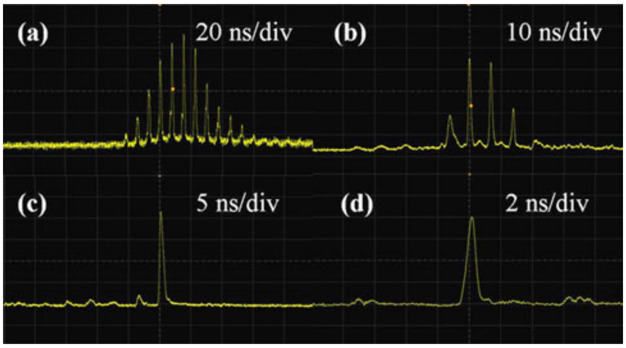

Fig. 4 Oscilloscope traces of the mode-locking pulse at different pump powers of **a** 2.75 W, **b** 4.03 W, **c** 4.65 W, and **d** 7.09 W

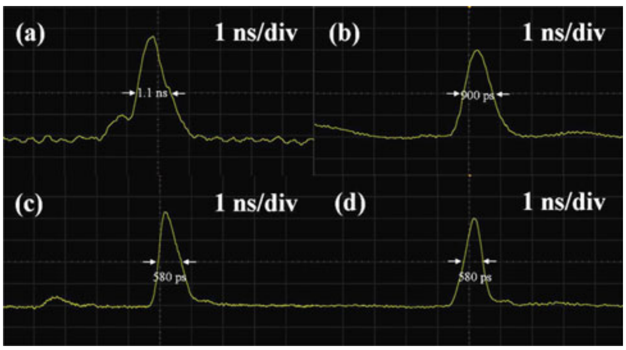

Fig. 5 Expanded images of the mode-locking pulse at different pump powers of **a** 2.75 W, **b** 4.03 W, **c** 4.65 W, and **d** 7.09 W

On the other hand, the number of the mode-locking pulses underneath the Q-switched envelope can be calculated according to the cavity round-trip time $2L'/c$ and the pulse width of the Q-switched envelope. When the pulse energy of the single Q-switched envelope is divided by the number of the mode-locking pulses, the average mode-locking pulse energy can be obtained [16], which is shown in Fig. 6. The experimental results show that an output coupler with transmission of T = 10 % can generate higher mode-locking pulse energy than the other cases. Furthermore, it also shows that mode-locking pulse energy was increased abruptly when single mode-locking pulse operation underneath one Q-switched envelope appeared. When the incident pump power was 8.25 W, a maximum mode-locking pulse energy of 582 μJ was achieved, which is much higher than those generated by Q-switched and mode-locking solid-state lasers [13, 14]. For the mode-locking pulse duration of 580 ps, the peak power of the mode-locking pulse was estimated to be as high as 1 MW.

Especially, because the repetition rate of single mode-locking pulse was controlled by the active modulator, this high peak power pulse laser with sub-nanosecond duration also has higher stability. Figure 7 shows the temporal pulse train recorded over 50 ms at the pump power of 8.25 W. The pulse to pulse amplitude fluctuation (the ratio between the largest deviation and the mean pulse amplitude) is only about 6 %. The experimental results show that the dual-loss-modulated technology is an efficient method to generate single mode-locking pulse with several KHz repetition rate and high stability.

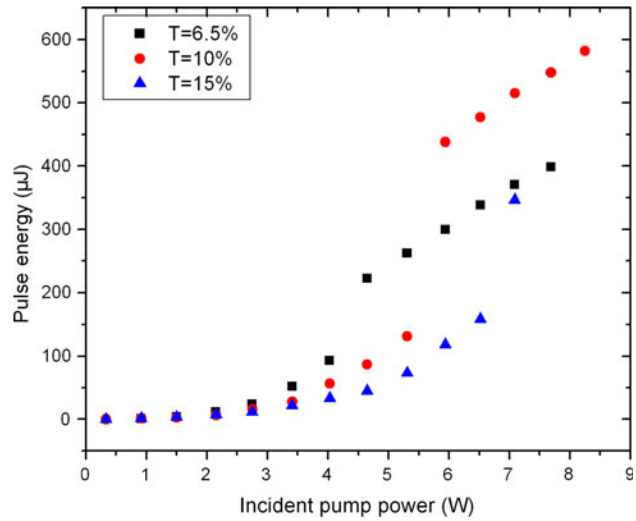

Fig. 6 Mode-locking pulse energy on the incident pump power

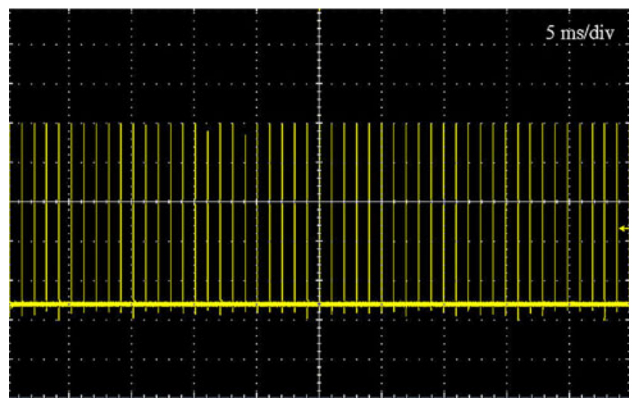

Fig. 7 Oscilloscope traces of a single mode-locking pulse train

3 Theoretical analysis

3.1 Theory of fluctuation mechanism

The generation of picosecond pulses in a simultaneously Q-switched and mode-locked laser with a saturable absorber could be explained by the fluctuation mechanism [20]. According to this mechanism, during the ultra-short pulse formation, there are the linear stage and the nonlinear stage including the nonlinear absorption and nonlinear amplification. In the linear stage of generation, the fluctuations of intensity arise owing to the interference of a great number of modes having a random phase distribution so that the radiation consists of a chaotic collection of ultrashort peaks. In the nonlinear stage, the most intensive fluctuation peaks are compressed and amplified faster than the weaker ones. When the pulse intensity rises beyond the saturation intensity range of the absorber, the preferred pulses will not be much further shortened on sequent round trips. During the linear stage and the nonlinear absorption, it is difficult to give the quantitatively theoretical description. Only in the nonlinear amplification process, because the pulse shape is not compressed, can the photon intensity shape be mathematically given [21, 22]. Especially, for LD-pumped QML laser with saturable absorber, the oscillating laser intensity is a Gaussian spatial distribution. In order to accurately describe the dynamics of the mode-locked laser, the Gaussian spatial distribution of the intracavity photon intensity can be written by introducing a coefficient of the Gaussian spatial distribution $\exp(-2r^2/w_1^2)$, where r is the distance from the axis in a Gaussian beam. Therefore, under Gaussian spatial distribution approximation, the average photon intensity shape in the nonlinear amplification process can be described as the form [21, 22]:

$$\begin{aligned}\varphi(r,t) &= \sum_{k=0} \Phi_k f(t-t_k)\exp\left(-\frac{2r^2}{w_1^2}\right) \\ &= \varphi(0,t)\exp\left(-\frac{2r^2}{w_1^2}\right)\end{aligned} \tag{1}$$

where $\varphi(0,t) = \sum_{k=0} \Phi_k f(t-t_k)$, $t_k = kt_r$, Φ_k is the relative amplitude of the mode-locked pulses at the kth round trip, $t_r = \frac{2[n_1 l + n_2 l_A + n_3 d + (L_p - l - l_A - d)]}{c}$ is the cavity round-trip time, and n_1, n_2, and n_3 are the refractive indices of the gain medium, the passive saturable absorber (GaAs wafer) and the active modulator (EO), respectively. l, l_A, and d are the lengths of the gain medium, GaAs wafer and the EO modulator, respectively, L_p is the physical length of the cavity. $f(t)$ is the mode-locked pulse evolving from the noise and satisfies $\int_{-\infty}^{\infty} c\sigma f(t)dt = 1$. $f(t)$ can be considered to be a hyperbolic secant function and written as [20]:

$$f(t) = \frac{1}{2\sigma c\tau_p} sh^2(t/\tau_p) \tag{2}$$

here, σ is the stimulated emission cross-section of the gain medium, and τ_p is related to the mode-locking pulse duration τ by $\tau = 1.76\tau_p$.

Thus the temporal Gaussian shape of the average photon intensity for the pulse at the kth round trip can be given by

$$\varphi_k(r,t) = \Phi_k f(t)\exp(-2r^2/w_1^2) \tag{3}$$

3.2 Rate equations and numerical simulation

Using the rate equation method, in which the Gaussian spatial distribution of the intracavity photon intensity, the influences of continuous pump rate, the stimulated radiation lifetime of the active medium, the excited-state lifetime of the saturable absorber and the loss of EO modulator are considered, the coupled rate equations for a diode-pumped dual-loss-modulated QML YVO_4/Nd:YVO_4 laser with EO and GaAs can be described as [22]:

$$\begin{aligned}\frac{d\varphi(0,t)}{dt} = \frac{2}{\pi w_1^2}\int_0^\infty \frac{1}{t_r}\Big\{&2\sigma n(r,t) l\varphi_G(r,t) - 2\sigma^+ n^+(r,t) l_A\varphi_A(r,t) \\ &-2\sigma^0[n_0 - n^+(r,t)]l_A\varphi_A(r,t) - Bl_A\varphi_A^2(r,t) \\ &-\left[L + \delta_e + \ln\left(\frac{1}{R}\right)\right]\varphi(r,t)\Big\}2\pi r dr\end{aligned} \tag{4}$$

$$\frac{dn(r,t)}{dt} = R_{in}(r) - \sigma c n(r,t)\varphi_G(r,t) - \frac{n(r,t)}{\tau_a} \tag{5}$$

$$\frac{dn^+(r,t)}{dt} = \sigma^0 c[n_0 - n^+(r,t)]\varphi_A(r,t) - \sigma^+ c n^+(r,t)\varphi_A(r,t) \tag{6}$$

here, $n(r,t)$ is the average population inversion density, n_0 is the total population density of the EL2 defect level of GaAs, $n^+(r,t)$ is the population density of positively charged $EL2^+$ in GaAs, σ^0 and σ^+ are the absorption cross-section of $EL2^0$ and $EL2^+$ in GaAs, R is the reflectivity of the output mirror, L is the intrinsic optical loss, which can be experimentally measured with the method in the Ref. [23]. $B = 6\beta h\nu c(w_G/w_A)^2$ is the coupling coefficient of two-photon absorption in GaAs, and β is the absorption coefficient of two photons, $R_{in}(r) = \frac{2\alpha P_{in}\exp(-2r^2/w_p^2)[1-\exp(-\alpha l)]}{h\nu_p \pi w_p^2 l}$ is the pump rate, where P_{in} is the pump power, $h\nu_p$ is the single-photon energy of the pump light, w_p is the average radius of the pump beam, and α is the absorption coefficient of the gain medium. δ_e is the loss of the EO modulator, τ_a is the emission lifetime of the upper laser level of the YVO_4/Nd:YVO_4 crystal. $\varphi_G(r,t)$ and $\varphi_A(r,t)$ are the photon densities at the positions of gain medium and GaAs wafer, respectively, and can be given as:

$$\varphi_i(r,t) = (w_l^2/w_i^2)\varphi(0,t)\exp(-2r^2/w_i^2)(i = G, A) \tag{7}$$

Substituting (1) into (7), the temporal shape of the photon intensity of the different positions at the kth round trip can be given as:

$$\phi_{k,i}(r,t) = (w_l^2/w_i^2)\exp(-2r^2/w_i^2)\Phi_k f(t)(i = G, A) \tag{8}$$

For the doubly QML laser, the relative amplitude of the mode-locking pulses will vary after each round trip. In the nonlinear amplification process, because the width of the mode-locking pulse is unaltered, the relative amplitude of the mode-locking pulses after an additional round trip through the laser meets the following relation:

$$\frac{\mathrm{d}\phi(0,t)}{\mathrm{d}t}=\phi(0,t)\frac{\mathrm{d}\ln\phi(0,t)}{\mathrm{d}t}=\phi(0,t)\frac{\Delta\ln\phi(0,t)}{\Delta t} \quad (9)$$

Using (1) and $t_k = kt_r$, it can be obtained that

$$\frac{\mathrm{d}\phi(0,t)}{\mathrm{d}t}=\frac{\phi(0,t)}{t_\mathrm{r}}\frac{\Delta\ln\phi(0,t)}{\Delta m}=\frac{\phi(0,t)}{t_\mathrm{r}}\ln\left(\frac{\Phi_k}{\Phi_{k-1}}\right) \quad (10)$$

Substituting (8) and (10) into (4), the recurrence relation of the relative amplitude for diode-pumped doubly QML YVO_4/Nd:YVO_4 laser with EO modulator and GaAs saturable absorber can be obtained as (11), where $n(r,t_k)$ and $n^+(r,t_k)$ are the population inversion density of the gain medium and the population density of positively charged $EL2^+$ in GaAs at the kth round trip, respectively.

$$\begin{aligned}\Phi_k=\Phi_{k-1}\exp\Bigg\{\frac{2}{\pi w_l^2}\int_0^\infty\Bigg[&2\sigma n(r,t_k)l\frac{w_\mathrm{l}^2}{w_\mathrm{G}^2}\exp\left(-\frac{2r^2}{w_\mathrm{G}^2}\right)\Bigg]\\&-2\sigma^+n^+(r,t_k)l_\mathrm{A}\frac{w_\mathrm{l}^2}{w_\mathrm{A}^2}\exp\left(-\frac{2r^2}{w_\mathrm{A}^2}\right)\\&-2\sigma^0[n_0-n^+(r,t_k)]l_\mathrm{A}\frac{w_\mathrm{l}^2}{w_\mathrm{A}^2}\exp\left(-\frac{2r^2}{w_\mathrm{A}^2}\right)\\&-Bl_\mathrm{A}\frac{w_\mathrm{l}^4}{w_\mathrm{A}^4}\exp\left(-\frac{4r^2}{w_\mathrm{A}^2}\right)\Phi_{k-1}\\&-\left[L+\delta_\mathrm{e}+\ln\left(\frac{1}{R}\right)\exp\right]\left(-\frac{2r^2}{w_\mathrm{l}^2}\right)2\pi r\,\mathrm{d}r\Bigg\}\end{aligned} \quad (11)$$

Substituting (1) and (8) into (5) and (6), and integrating the results over time from zero to t_k, (12) and (13) can be obtained.

$$\begin{aligned}n(r,t_k)=\exp\left(-\frac{t_k}{\tau_a}\right)\prod_0^{k-1}\exp\left[-\frac{w_\mathrm{l}^2}{w_\mathrm{G}^2}\exp\left(-\frac{2r^2}{w_\mathrm{G}^2}\right)\Phi_\mathrm{m}\right]\\\times\Bigg\{R_\mathrm{in}(r)\exp\left(\frac{t_k}{\tau_a}\right)\int_0^{t_k}\prod_{m=0}^{k-1}\exp\left[\frac{w_\mathrm{l}^2}{w_\mathrm{G}^2}\exp\left(-\frac{2r^2}{w_\mathrm{G}^2}\right)\Phi_\mathrm{m}\right]\mathrm{d}t\\+n_i\exp\left(-\frac{2r^2}{w_\mathrm{p}^2}\right)\Bigg\}\end{aligned} \quad (12)$$

$$\begin{aligned}n^+(r,t_k)=\left[\prod_{m=0}^{k-1}\exp\left[-\frac{w_l^2}{w_A^2}\exp\left(-\frac{2r^2}{w_A^2}\right)\Phi_m\right]\right]^{(\sigma^++\sigma^0)/\sigma}\\\times\Bigg\{\int_0^k\left[\prod_{m=0}^{k-1}\exp\left[\frac{w_l^2}{w_A^2}\exp\left(-\frac{2r^2}{w_A^2}\right)\Phi_m\right]\right]^{(\sigma^++\sigma^0)/\sigma}\\\times\frac{\sigma^0n_0}{2\sigma\tau_p}\times\sum_{m=0}^{k-1}\Phi_m\frac{w_l^2}{w_A^2}\exp\left(-\frac{2r^2}{w_A^2}\right)\sec h^2\left(\frac{t-mt_\gamma}{\tau_p}\right)dt+n_0\Bigg\}\end{aligned} \quad (13)$$

Using the parameters shown in Table 1, for a given initial value of Φ_0, by numerically solving (11)–(13), Φ_k can be obtained. The initial population inversion density for doubly QML laser can be expressed as [24]:

$$n_i=R_\mathrm{in}\tau_\mathrm{a}[1-\exp(-1/f_\mathrm{p}\tau_\mathrm{a})] \quad (14)$$

where f_p is the modulation frequency of EO. Meanwhile, the output power coupled out of the cavity can be expressed as:

$$P(t)=\frac{h\nu\pi w_\mathrm{l}^2}{8\sigma\tau_\mathrm{p}}\left(\ln\frac{1}{R}\right)\sum_{k=0}^{\infty}\phi_k\sec h^2\left(\frac{t-t_k}{\tau_\mathrm{p}}\right) \quad (15)$$

Based on the above equations, the calculated temporal shape of the mode-locking pulses at pump power of 2.75, 4.03, 4.65, and 7.09 W can be obtained, which are shown in Fig. 8.

By integrating (15) over time from zero to infinity, the total output energy of the QML pulse can be obtained as

Table 1 Parameters of the theoretical calculation

Parameters	Values	Parameters	Values
σ	2.5×10^{-18} cm^2	l_A	0.7 mm
σ^0	1.0×10^{-16} cm^2	d	50 mm
σ^+	2.3×10^{-17} cm^2	c	3×10^8 ms^{-1}
n^0	1.2×10^{16} cm^{-3}	n_1	2.183
n^+	1.4×10^{15} cm^{-3}	n_2	3.48
w_p	400 µm	n_3	1.65
w_l	200 µm	β	2.6×10^{-8} cm W^{-1}
w_G	206 µm	δ_e	0.1
w_A	132 µm	α	5.32 cm^{-1}
τ_a	98 µs	L	0.09
τ_p	200 ps	l	8 mm

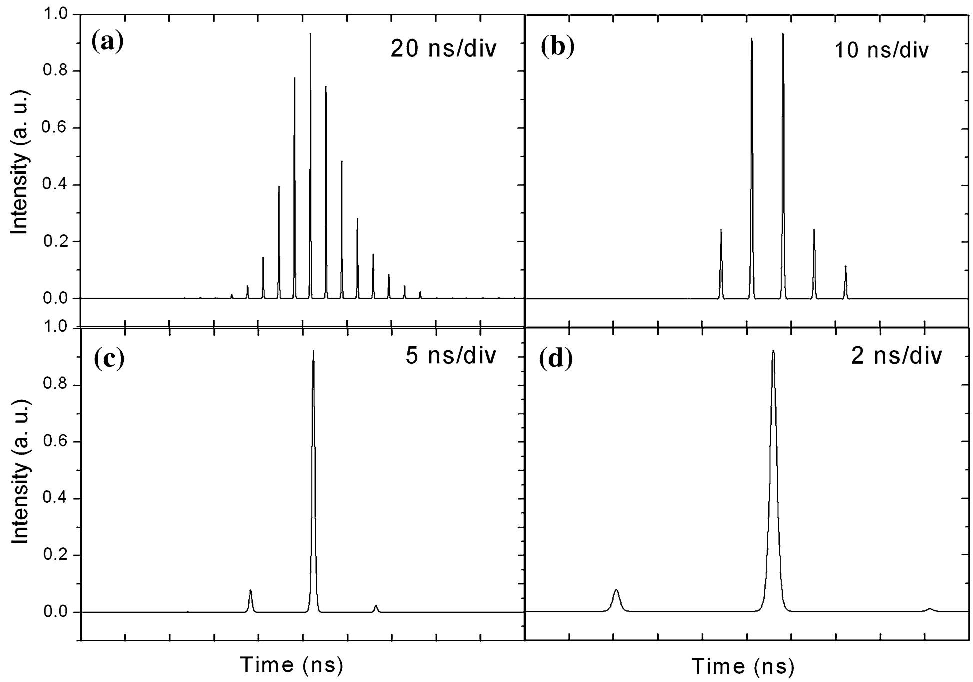

Fig. 8 Calculated temporal shape of the mode-locking pulse at different pump powers of **a** 2.75 W, **b** 4.03 W, **c** 4.65 W, and **d** 7.09 W

$$E = \frac{h\nu\pi w_l^2}{8\sigma}\left(\ln\frac{1}{R}\right)\sum_{k=0}^{\infty}\phi_k \quad (16)$$

Through this method, the results of theoretical calculations were obtained, as shown with the solid curve in Figs. 2, 3. From the figures, it can be seen that the theoretical evaluations are basically in accordance with the experimental results.

4 Conclusion

In conclusion, a diode-pumped doubly QML YVO_4/Nd:YVO_4 laser with EO and GaAs at 1.06 μm is presented. Under the fixed conditions, stable single mode-locking pulses with repletion rate of 1 kHz and duration of 580 ps were generated. A maximum peak power of the mode-locking pulse is estimated to be as high as 1 MW. The experimental results demonstrate a novel and simple method to generate picosecond pulses at low repetition rates. Using a hyperbolic secant square function and considering the Gaussian distribution of the intracavity photon density, the coupled equations for diode-pumped dual-loss-modulated QML YVO_4/Nd:YVO_4 laser are given, and the numerical solutions of the equations are basically in accordance with the experimental results.

Acknowledgments This work is partially supported by the National Science Foundation of China (61078031), the National Science Foundation of China for Youths (61205145, 61008024), the Natural Science Foundation of Shandong Province (ZR2011FM012), the Science and Technology Development Program of Shandong Province (2012G 0020126), the China Postdoctoral Science Foundation (2012M511024), the Research Award Fund for Outstanding Middle-aged and Young Scientist of Shandong Province (BS2011DX022) and the Independent Innovation Foundation of Shandong University (2012JC025).

References

1. S. Lévêque-Fort, D.N. Papadopoulos, S. Forget, F. Balembois, P. Georges, Opt. Lett. **30**, 168 (2005)
2. P.G. Antal, R. Szipocs, Appl. Phys. B **107**, 17 (2012)
3. H. Sayinc, D. Mortag, D. Wandt, J. Neumann, D. Kracht, Opt. Express **17**, 5731 (2009)
4. F. Dausinger, H. Hügel, V. Konov, Proc. SPIE **5147**, 106 (2003)
5. A. Agnesi, L. Carra, F. Pirzio, G. Reali, A. Tomaselli, D. Scarpa, C. Vacchi, IEEE J. Quantum Electron **42**, 772 (2006)
6. K.H. Fong, S.Y. Kim, K. Kikuchi, H. Yaguchi, S.Y. Set, Optical amplifiers and their applications/coherent optical technologies and applications, OSA technical digest series(CD) (Optical Society of America, 2006), paper OMD4
7. J. Xu, Y. Yang, J. He, B. Zhang, X. Yang, S. Liu, B. Zhang, H. Yang, IEEE J. Quantum Electron **48**, 622 (2012)
8. W.B. Cho, A. Schmidt, S.Y. Choi, V. Petrov, U. Griebner, G. Steinmeyer, S. Lee, D. Yeom, F. Rotermund, Opt. Lett. **35**, 2669 (2010)
9. J. Jabczynski, W. Zendzian, J. Kwiatkowski, Opto-Electron Rev. **14**, 135 (2006)
10. V.Z. Kolev, M.J. Lederer, B. Luther-Davies, A.V. Rode, Opt. Lett. **28**, 1275 (2003)
11. S. Kobtsev, S. Kukarin, Y. Fedotov, Opt. Express **16**, 21936 (2008)
12. J.C. Balzer, T. Schlauch, Th Hoffmann, A. Klehr, G. Erbert, M.R. Hofmann, Electron Lett. **47**, 1387 (2011)
13. C. Theobald, M. Weitz, R. Knappe, R. Wallenstein, J.A. L' Huillier, Appl. Phys. B **92**, 1 (2008)
14. J.-H. Lin, K.-H. Lin, H.-H. Hsu, W.-F. Hsieh, Laser Phys. Lett. **5**, 276 (2008)

15. S. Zhao, G. Li, D. Li, K. Yang, Y. Li, M. Li, T. Li, K. Cheng, G. Zhang, H. Ge, Laser Phys. Lett. **7**, 29 (2010)
16. T. Li, S. Zhao, Z. Zhuo, K. Yang, G. Li, D. Li, Opt. Express **18**, 10315 (2010)
17. K. Nawata, M. Okida, K. Furuki, T. Omatsu, Opt. Express **15**, 9123 (2007)
18. R.A. Fields, M. Birnbaum, C.L. Fincher, Appl. Phys. Lett. **51**, 1885 (1987)
19. Z. Zhuo, T. Li, X. Li, H. Yang, Opt. Commun. **274**, 176 (2007)
20. P.K. Mukhopadhyay, M.B. Alsousb, K. Ranganathan, S.K. Sharma, P.K. Gupta, J. George, T.P.S. Nathan, Appl. Phys. B **79**, 713 (2004)
21. Y.F. Chen, J.L. Lee, H.D. Hsieh, S.W. Tsai, IEEE J. Quantum Electron **38**, 312 (2002)
22. K. Yang, S. Zhao, G. Li, M. Li, D. Li, J. Wang, J. An, IEEE J. Quantum Electron **42**, 683 (2006)
23. R.C. Stoneman, L. Esterowitz, IEEE J. Sel. Top. Quant. **1**, 78 (1995)
24. T. Li, Ph.D dissertation, Opt. Eng., Shandong Univ., Jinan, China, 2010